©SHUTTERSTOCK/ JARTEE

Circuit AI for Bill of Materials, Switching Loss Optimization, Capacitor RMS Estimation, and More

by Vishwam Raval, Mohamed Zeid, Prasad Enjeti, and Grant Pitel

Digital Object Identifier 10.1109/MPEL.2024.3524782
Date of publication: 25 February 2025

This article details the development of a bill of materials (BOM) tool, Circuit AI, which integrates with OpenAI's GPT-4 model to streamline component selection and optimization in electronic design. Circuit AI leverages GPT-4's Function Calling, Code Interpreter, and fine-tuning capabilities to simplify BOM tasks, such as switching loss optimization and capacitor RMS estimation. By automating tedious searches for components, availability, and datasheets, engineers can focus on critical design work and make informed decisions on cost-effective, reliable parts (Figure 1). Tested with a Texas Instruments BOM, Circuit AI demonstrated its efficiency in optimizing reference designs, identifying alternatives, and enhancing workflows from selection to production. A key application of Circuit AI is in power electronics, where it leverages GPT-4's fine-tuning capabilities to estimate capacitor RMS currents ($I_{cap\text{-}rms}$), a crucial factor in preventing overheating and potential failure.

Engineers rely on tools like Altium [4] to generate schematics and compile comprehensive BOM for their designs, detailing semiconductors, ICs, and passive components. However, sourcing specific components, verifying part numbers, checking costs and availability, and reviewing datasheets from distributors like Mouser [1] and DigiKey [2] is a time-consuming and tedious process. The challenge is exacerbated when components reach end of life (EOL), requiring engineers to manually search for replacements—a task that delays progress and detracts from design refinement.

To address these inefficiencies, we present Circuit AI, powered by OpenAI's GPT-4 Function Calling [3]. This innovative solution streamlines component searches, delivering instant results and enabling engineers to focus on design optimization. Whether integrated with Altium or other design tools, Circuit AI accelerates development by simplifying critical workflows.

Key advantages of Circuit AI include:

a) Automated Component Search: Quickly retrieves part details, availability, cost, and datasheets from sources like Mouser [1] and DigiKey [2].
b) Datasheet Parsing: Extracts critical specs such as MOSFET $R_{ds\text{-}on}$ rise time t_r and fall time t_f for immediate use in calculations, switching losses.
c) Real-Time Calculations: Executes Python code to compute using the Code Interpreter. This facilitates --- complex circuit analyses, rapid design optimization, component comparisons, and precise parameter tuning directly within the workflow, saving time and reducing errors.
d) BOM Optimization: using Circuit AI one can determine cost-effective alternatives as well as identify parts from preferred manufacturers.
e) Web Integration: Searches the web for the latest datasheets and research.

The sections below explain the construction of Circuit AI with the Chat GPT 4o employing the function calling, file search and code interpreter features.

Function Calling Feature Explained

OpenAI's Function Calling [3] feature enhances the capabilities of GPT models by enabling them to interact directly with external tools and APIs. This functionality allows natural language queries to be converted into precise function calls, enabling the retrieval of structured data or the execution of specific actions. In the context of electronic component searches, this capability transforms the traditionally manual process into an automated, efficient workflow.

In this section, we describe the design of a specific function calling feature. As shown in Figure 1, OpenAI's function calling is connected to the Mouser/Digikey Search API [2], [5] via a local self-hosted Node.js server. This integration allows the tool to automatically pull key information about components—such as cost, availability, and datasheets—based on the BOM. To demonstrate the implementation of function calling on the assistant side, a JSON Schema provided to the assistant as a

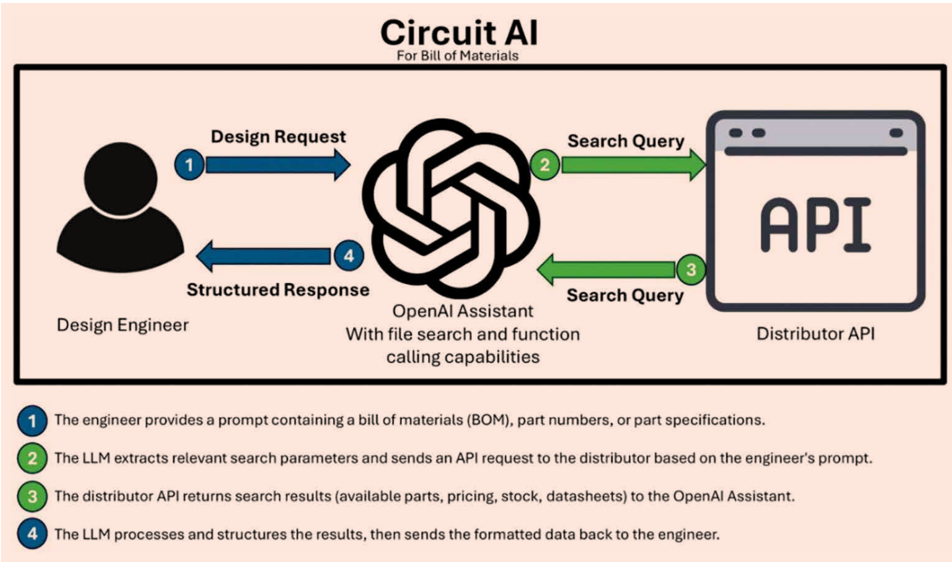

FIG 1 Circuit AI for BOM: Streamlining part searches by automating bill of materials queries. The system processes engineer requests, retrieves data from distributor APIs, and returns structured results for efficient design decisions.

```
{
  "name": "searchMouser",
  "description":
"Search for electronic components on Mouser and return the res
ults with name, availibility, mouser part number, datasheet, m
anufacturer and part image"
,
  "strict": false,
  "parameters": {
    "type": "object",
    "properties": {
      "searchquery": {
        "type": "string",
        "description":
"The search query for the electronic component, e.g., 'LM317 r
egulator'"
      }
    },
    "required": [
      "searchquery"
    ]
  }
}
```

FIG 2 JSON Schema for defining function for OpenAI 4o model Assistant API.

one-time input from the developer to allow the LLM to know that there exists a defined function to search for parts in Figure 2.

The function "searchMouser" is defined with a required "searchquery" parameter, which expects a search string (e.g., "LM317 Regulator"). When a user requests a component lookup, the model identifies the specific part and makes a structured API call to external sources like Mouser. This call retrieves the latest information on stock levels, pricing, and datasheets, delivering the data instantly back to the user. To connect the Assistant session to the API, the "handleRequiresAction" function in Figure 3a, takes in the run id and thread id and checks if the current run id requires any tool (Figure 3b) to complete the request. Once the request is identified, it makes a function call using the assistant tools.

If the required tool name is "searchMouser", then it sends the Mouse Search API a request with the identified search query, and formats the response as a string. The output is then sent back to the run id and thread session to complete the user's request.

Identifying Components in BOM With Gen-AI

To showcase the functionality of the Circuit AI for BOM, let's examine a real-world example: the PMP10532 Isolated Tri-output Fly-Buck Power Supply [7] (Figure 4) for industrial PLC applications, designed by Texas Instruments (see Table 1a). This example highlights how function calling capabilities can streamline the process of identifying components in the BOM.

The Model was able to extract the parts from the BOM, find them on Mouser and find their alternatives accurately (Table 1b).

```
async function handleRequiresAction(run, thread) {
  if (
    run.required_action &&
    run.required_action.submit_tool_outputs &&
    run.required_action.submit_tool_outputs.tool_calls
  ) {
    const toolOutputs = await Promise.all(
      run.required_action.submit_tool_outputs.tool_calls.map(
async (tool) => {
        console.log("Tool function:", tool.function);
        if (tool.function.name === "searchMouser") {
          const functionArguments = JSON.parse(tool.function.
arguments);
          const searchResults = await searchMouser(
            functionArguments.searchquery,
          );
          return {
            tool_call_id: tool.id,
            output: JSON.stringify(searchResults),
          };
        }
        if (tool.function.name === "addToMouserCart") {
          const functionArguments = JSON.parse(tool.function.
arguments);
          const cartResponse = await addToMouserCart(
            functionArguments.CartItems,
          );
          return {
            tool_call_id: tool.id,
            output: JSON.stringify(cartResponse),
          };
        }
        if (tool.function.name === "searchDigikey") {
          const functionArguments = JSON.parse(tool.function.
arguments);
          const searchResults = await searchDigikey(
            functionArguments.searchquery,
          );
          return {
            tool_call_id: tool.id,
            output: JSON.stringify(searchResults),
          };
        }
      }),
    );

    if (toolOutputs.length > 0) {
      run = await openai.beta.threads.runs.
submitToolOutputsAndPoll(
        thread.id,
        run.id,
        { tool_outputs: toolOutputs.filter((output) => output
!== undefined) },
      );
    } else {
      console.log("No tool outputs to submit.");
    }
    return handleRunStatus(run, thread);
  }
}
```

(a)

```
async function handleRunStatus(run, thread) {
  if (run.status === "completed") {
    const messages = await openai.beta.threads.messages.list(
thread.id);
    return messages.data.find((message) => message.role ===
"assistant")
      .content;
  } else if (run.status === "requires_action") {
    return await handleRequiresAction(run, thread);
  } else {
    console.error("Run did not complete:", run);
  }
}
```

(b)

FIG 3 JavaScript code on the server-side of Circuit AI. (a) Handling function calls when action is required. (b) Identifying and forwarding the requested task to appropriate actions for function calling.

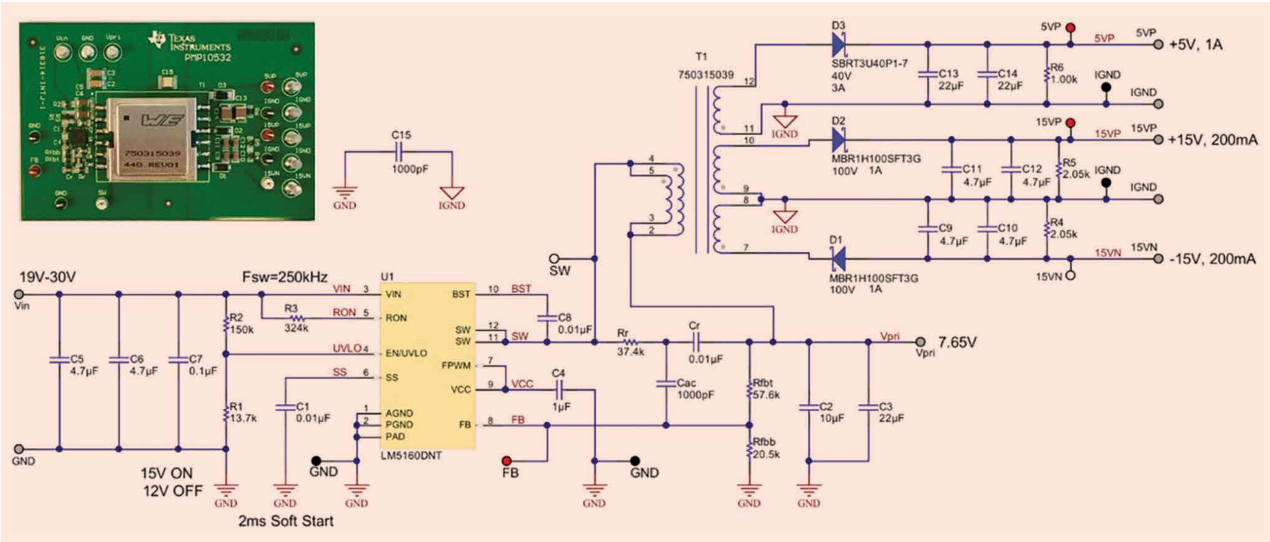

FIG 4 Texas instruments PMP10532 schematic and PCB for isolated tri-output Fly-Buck power supply for industrial PLC applications [7].

Prompting the Model to Look for Part Alternatives

In many cases, industrial manufacturers like Magna-Power Electronics [6] choose to source components from a preferred manufacturer that differs from what was suggested in the reference design. As an example, Item #12 on the TI BOM (refer to Table 1b) lists a 1000 pF 50 V X7R 0603 capacitor from TDK, and the preferred manufacturer is Vishay, the Circuit AI for Bill of Materials can be prompted to search for an alternative as:

It is clear from Figure 5 the correct replacement part for the capacitor from Vishay was successfully found from the Mouser database by the Circuit AI. Furthermore, part specifications along with the cost can also be extracted from the database. The tailored Circuit AI for Bill of Materials can also search for replacements by reviewing the top four results from the distributor's query and selecting the most affordable option as shown below in Figure 6:

Once all the components and quantities are finalized by the design engineer, they can prompt the tool to add them to their shopping cart, and the model can use the function calling feature to generate a cart on the distributor's website [5] (Figure 7).

The integration of OpenAI's Function Calling feature with external APIs, such as those from Mouser and DigiKey, marks a significant advancement in the design workflow for engineers. By automating the process of identifying components, checking availability, comparing prices, and accessing datasheets, the proposed Circuit AI for Bill of Materials reduces the manual effort required in compiling and verifying the Bill of Materials (BOM). This not only saves valuable time but also allows engineers to focus on critical design tasks, ensuring faster project completion and improved efficiency. As demonstrated with the PMP10532 Fly-Buck power supply example, this tool is a game-changer for power electronics and beyond, offering engineers an intuitive and reliable solution to streamline component searches, optimize cost-efficiency, and stay ahead in the competitive landscape of design engineering.

Calculating Switching and Conduction Losses for MOSFETs

In power electronics, accurately estimating switching and conduction losses in MOSFETs is crucial to optimize efficiency and thermal management in circuit designs. MOSFET losses primarily arise from two mechanisms: conduction losses, which occur when the device is on, and switching losses, which are incurred during transitions between on and off states. The Code Interpreter feature in Circuit AI allows for on-the-fly generation and execution of Python code in the backend to calculate switching and conduction losses for MOSFETs. This tool transforms the way engineers approach loss analysis, enabling them to quickly obtain results without manually coding the required calculations, as shown in Figure 8.

Switching Losses: Switching losses (P_{switch}) occur during the rise and fall times of the MOSFET as it transitions between its on and off states. These losses are calculated based on the energy dissipated during the switching events and can be expressed as [8]:

$$P_{\text{switch}} = \frac{1}{2} * V_{\text{ds}} * I_{\text{load}} * \left(t_r + t_f\right) * f_{\text{sw}} \qquad (1)$$

Where,

- V_{ds} is the drain-to-source voltage during the switching event.
- I_{load} is the current at the time of switching.
- t_r and t_f are the rise and fall times, respectively, typically found in the datasheet.
- f_{sw} is the switching frequency.

Table 1. (a) TI bill of materials for PMP10532 reference design. (b) LLM generated bill of materials for TI PMP10532 with the available parts and alternatives in stock on Mouser [1].

Texas Instruments

Bill of Materials

TI DESIGNS PMP10532

Item	Qty	Reference	Value	Part Description	Manufacturer	Manufacturer Part Number	PCB Footprint	Note
1	3	5VP2, 15VP2, FB	Red	Test Point, TH, Miniature, Red	Keystone	5000	Keystone5000	In Stock
2	8	5VP, 15VN, 15VP, GND, IGND, IGND2, Vin, Vpri		Double Terminal, Turret, TH, Double	Keystone	1502-2	Keystone1502-2	In Stock
3	2	15VN2, SW	White	Test Point, Miniature, White, TH	Keystone	5002	Keystone5002	In Stock
4	2	C1, C8	0.01uF	CAP, CERM, 0.01uF, 50V, +/-10%, X7R, 0603	TDK	C1608X7R1H103K	0603	In Stock
5	1	C2	10uF	CAP, CERM, 10uF, 25V, +/-10%, X7R, 1206	MuRata	GRM31CR71E106KA12L	1206	In Stock
6	3	C3, C13, C14	22uF	CAP, CERM, 22uF, 16V, +/-20%, X7R, 1210	TDK	C3225X7R1C226M	1210	In Stock
7	1	C4	1uF	CAP, CERM, 1uF, 25V, +/-10%, X7R, 0603	TDK	C1608X7R1E105K080AB	0603	In Stock
8	2	C5, C6	4.7uF	CAP, CERM, 4.7uF, 50V, +/-10%, X7R, 1206	MuRata	GRM31CR71H475KA12L	1206	In Stock
9	1	C7	0.1uF	CAP, CERM, 0.1uF, 50V, +/-10%, X7R, 0603	TDK	C1608X7R1H104K	0603	In Stock
10	4	C9, C10, C11, C12	4.7µF	CAP, CERM, 4.7uF, 25V, +/-20%, X7R, 0805	TDK Corporation	CGA4J1X7R1E475M125AC	0805	In Stock
11	1	C15	1000pF	CAP, CERM, 1000pF, 1000V, +/-10%, X7R, 1210	Vishay-Vitramon	VJ1210Y102KXGAT5Z	1210	In Stock
12	1	Cac	1000pF	CAP, CERM, 1000pF, 50V, +/-10%, X7R, 0603	TDK	C1608X7R1H102K	0603	Obsolete
13	1	Cr	0.01uF	CAP, CERM, 0.01uF, 50V, +/-10%, X7R, 0603	MuRata	GRM188R71H103KA01D	0603	Obsolete
14	2	D1, D2	100V	Diode, Schottky, 100V, 1A, SOD-123FL	ON Semiconductor	MBR1H100SFT3G	SOD-123FL	In Stock
15	1	D3	3A TrenchSBR 40Vrrm 3A Io	0.49Vf 180Ir	Diodes Incorporated	SBRT3U40P1-7	powerDI123	In Stock
16	4	GND2, GND3, IGND3, IGND4	Black	Test Point, TH, Miniature, Black	Keystone	5001	Keystone5001	In Stock
17	1	R1	13.7k	RES, 13.7k ohm, 1%, 0.1W, 0603	Vishay-Dale	CRCW060313K7FKEA	0603	In Stock
18	1	R2	150k	RES, 150k ohm, 1%, 0.1W, 0603	Vishay-Dale	CRCW0603150KFKEA	0603	In Stock
19	1	R3	324k	RES, 324k ohm, 1%, 0.1W, 0603	Yageo America	RC0603FR-07324KL	0603	In Stock
20	2	R4, R5	2.05k	RES, 2.05k ohm, 1%, 0.1W, 0603	Vishay-Dale	CRCW06032K05FKEA	0603	In Stock
21	1	R6	1.00k	RES, 1.00k ohm, 1%, 0.1W, 0603	Vishay-Dale	CRCW06031K00FKEA	0603	In Stock
22	1	Rfbb	20.5k	RES, 20.5k, 1%, 0.1W, 0603	Vishay-Dale	CRCW060320K5FKEA	0603	In Stock

Continued

Table 1. (a) TI bill of materials for PMP10532 reference design. (b) LLM generated bill of materials for TI PMP10532 with the available parts and alternatives in stock on Mouser [1]. (Continued)

23–	1	Rfbt	57.6k	RES, 57.6k, 1%, 0.1W, 0603	Vishay-Dale	CRCW060357K6FKEA	0603	In Stock
24	1	Rr	37.4k	RES, 37.4k, 1%, 0.1W, 0603	Vishay-Dale	CRCW060337K4FKEA	0603	In Stock
25	1	T1	40uH	Transformer, 45uH, Isat 2.5A, EFD20, 12 pin, SMT, 6:4:11:11	Wurth Elektronik	750315039	Wurth_ EFD20_12pin_SMT	In Stock
26	1	U1	Wide Input 65V, 1.5A	Synchronous Step-Down DC-DC Converter, DNT0012B	Texas Instruments	LM5160DNT	DNT0012B	In Stock

(a)

Item	Qty	Reference	Value	Part Description	Manufacturer	Price (per component)	Availability
1	3	5VP2, 15VP2, FB	Red	Test Point, TH, Miniature, Red	3825	$0.0995	In Stock
2	8	5VP, 15VN, 15VP, GND, IGND, IGND2, Vin, Vpri	Double	Terminal, Turret, TH, Double	1573-1	$0.32	In Stock
3	2	15VN2, SW	White	Test Point, Miniature, White, TH	105-0858-001	$2.29	In Stock
4	2	C1, C8	0.01uF	CAP, CERM, 0.01uF, 50V, +/-10%, X7R, 0603	0402X7R103KTAT	$0.26	In Stock
5	1	C2	10uF	CAP, CERM, 10uF, 25V, +/-10%, X7R, 1206	CGA5L1X7R1E106K160AC	$0.54	In Stock
6	3	C3, C13, C14	22uF	CAP, CERM, 22uF, 16V, +/-20%, X7R, 1210	C3225X7R1C226M250AC	$0.57	In Stock
7	1	C4	1uF	CAP, CERM, 1uF, 25V, +/-10%, X7R, 0603	CM105X7R105K25AT	$0.24	In Stock
8	2	C5, C6	4.7uF	CAP, CERM, 4.7uF, 50V, +/-10%, X7R, 1206	C2012X7R1H475K125AE	$0.65	In Stock
9	1	C7	0.1uF	CAP, CERM, 0.1uF, 50V, +/-10%, X7R, 0603	CC0603JRX7R9BB104	$0.10	In Stock
10	4	C9, C10, C11, C12	4.7uF	CAP, CERM, 4.7uF, 25V, +/-20%, X7R, 0805	C3216X7R1E475M160AE	$0.65	In Stock
11	1	C15	1000pF	CAP, CERM, 1000pF, 1000V, +/-10%, X7R, 1210	C1206C102KDRAC	$0.14	In Stock
12	1	Cac	1000pF	CAP, CERM, 1000pF, 50V, +/-10%, X7R, 0603	K102M15X7RF53L2	$0.16	In Stock
13	1	Cr	0.01uF	CAP, CERM, 0.01uF, 50V, +/-10%, X7R, 0603	0402X7R103KT2AT	$0.26	In Stock
14	2	D1, D2	100v	Diode, Schottky, 100v, 1A, SOD-123FL	SS1H10-E3/61T	$0.37	In Stock
15	1	D3	-	Diodes Inc. 3A TrenchSBR 40Vrrm 3A Io 0.49Vf 180Ir	SBRT3M40P1-7	$0.40	In Stock
16	4	GND2, GND3, IGND3, IGND4	Black	Test Point, TH, Miniature, Black	105-0771-001	$1.15	In Stock
17	1	R1	13.7kOhm	RES, 13.7k ohm, 1%, 0.1W, 0603	RK73H1ETTP1372F	$0.10	In Stock
18	1	R2	150kOhm	RES, 150k ohm, 1%, 0.1W, 0603	ERJ-H2RD1503X	$0.29	In Stock
19	1	R3	324kOhm	RES, 324k ohm, 1%, 0.1W, 0603	RK73H1ETTP3243F	$0.10	In Stock
20	2	R4, R5	2.05kOhm	RES, 2.05k ohm, 1%, 0.1W, 0603	RK73H1ETTP2051F	$0.10	In Stock
21	1	R6	1.00kOhm	RES, 1.00k ohm, 1%, 0.1W, 0603	CRCW06031K00FKEAC	$0.10	In Stock

Continued

Table 1. (a) TI bill of materials for PMP10532 reference design. (b) LLM generated bill of materials for TI PMP10532 with the available parts and alternatives in stock on Mouser [1]. (Continued)

22	1	Rfbb	20.5kOhm	RES, 20.5k, 1%, 0.1W, 0603	RK73H1ETTP2052F	$0.10	In Stock
23	1	Rfbt	57.6kOhm	RES, 57.6k, 1%, 0.1W, 0603	RK73H1ETTP5762F	$0.10	In Stock
24	1	Rr	37.4kOhm	RES, 37.4k, 1%, 0.1W, 0603	RK73H1ETTP3742F	$0.10	In Stock
25	1	T1	40uH	Transformer, 45uH, Isat 2.5A, EFD20, 12 pin, SMT, 6:4:11:11	750314462	$4.78	In Stock
26	1	U1	-	Wide Input 65V, 1.5A Synchronous Step-Down DC-DC Converter, DNT0012B	LM5160DNTT	$5.58	In Stock

(b)

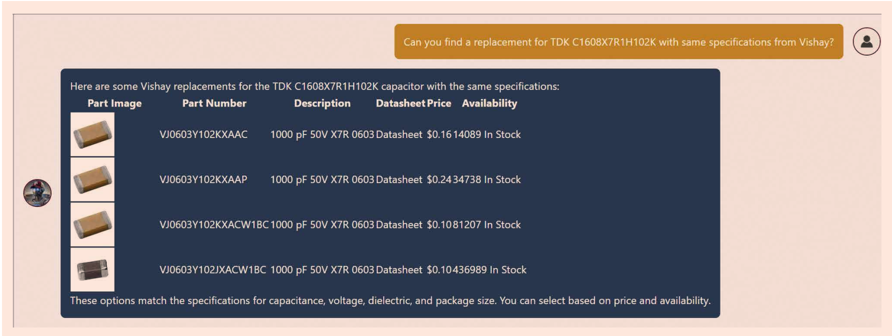

FIG 5 Screenshot of Circuit AI in action: effortlessly sourcing component alternative with language prompts with manufacturer preferences.

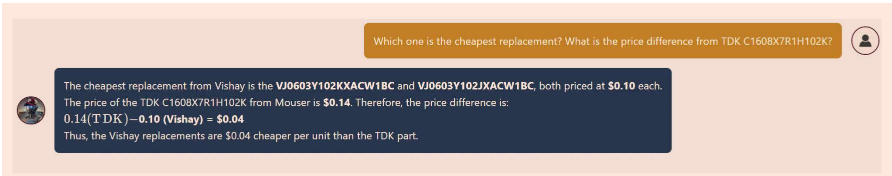

FIG 6 Cost effectiveness by picking a different component.

FIG 7 Screenshot of Circuit AI in action: Generating a cart for the TI PMP10532 bill of materials with the Circuit AI suggested parts on Mouser [1] using language prompt and API interactions.

1) Conduction Losses: Conduction losses (P_{cond}) depend on the MOSFET's on-state resistance ($R_{ds\text{-}on}$) and the current flowing through the device. This can be computed using the following equation [8]:

$$P_{cond} = I_{rms}^{2} * R_{ds\text{-}on} \quad (2)$$

Where,

- I_{lrms} is the root mean square current through the MOSFET.
- $R_{ds\text{-}on}$ is the MOSFET's on-resistance, typically found in the datasheet.

The conduction losses are directly proportional to both the square of the current and the on-resistance. By automating the retrieval of MOSFET datasheets through

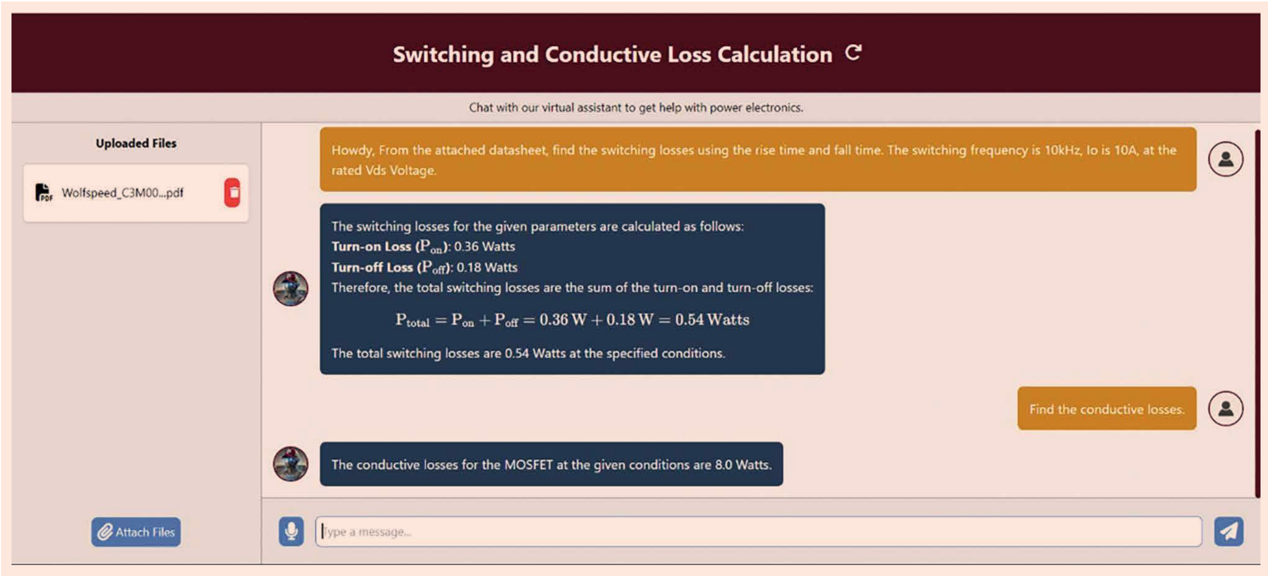

FIG 8 Screenshot of Circuit AI in action: Language prompt to calculate ideal switching and conduction losses for Wolfspeed C3M0065090J MOSFET.

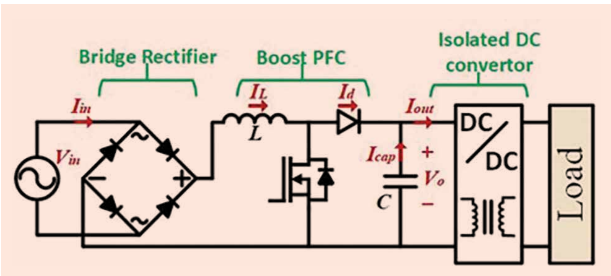

FIG 9 Circuit topology of a typical switching power supply with a PFC stage [3], each of the different variables are indicated on the diagram and the variable of interest is I_{cap}.

GenAI, engineers can streamline this calculation process. Circuit AI, for example, can extract $R_{ds\text{-}on}$ from the component datasheet, making it easier to compute conduction losses across different MOSFET options.

GenAI models can automate the extraction of parameters from the datasheets and directly compute switching and conductive losses using (1) and (2) across different operating conditions. By integrating these calculations, engineers can quickly compare multiple MOSFETs and determine which devices offer the best trade-off between switching speed and efficiency, ultimately minimizing system losses.

Circuit AI Operation Details

Circuit AI's usage cost structure is based on three components. First, the flagship model (OpenAI GPT-4o) currently charges U.S. $2.50 per one million input tokens and U.S. $10.00 per one million output tokens. Second, the code interpreter costs U.S. $0.03 per session. Third, file search with vector storage charges U.S. $0.10 per GB of data stored daily. The demonstration of Circuit AI would cost around U.S. $0.05 for the session. The system works by charging for token usage (input/output text chunks), code interpretation sessions, and the amount of vectorized data stored and searched, making costs proportional to usage.

Capacitor RMS Estimation in Single Phase Power Factor Correction Circuits

One notable application of Circuit AI in power electronics is its ability to estimate circuit behavior across various setups. Figure 9 illustrates a power factor correction (PFC) circuit schematic, highlighting I_{cap}—the capacitor current—as a critical factor. The rms capacitor current $I_{cap\text{-}rms}$ is responsible for capacitor heating and subsequent degradation leading to failure of PFC circuits [10]. Therefore, it is important to estimate $I_{cap\text{-}rms}$ for various input voltage/output load conditions. This capability is especially crucial in high-reliability systems such as data centers, where each server power supply consists of a PFC stage followed by a dc-dc converter stage. Unplanned downtime due to capacitor failure is unacceptable. The root-mean-square (RMS) current, $I_{cap\text{-}rms}$, can be calculated using equation [3] below, based on input voltage (V_{in}) and current (I_{in}), output voltage (V_o), and associated harmonics. For a detailed derivation, consult the Rectifiers and Inverters class notes [10]

$$I_{cap} = \frac{V_{in} * I_{in}}{V_o} \cos(2wt) + \text{Higher Order Terms.} \qquad (3)$$

To tailor the LLM for accurate $I_{cap\text{-}rms}$ current prediction, data was gathered across multiple PFC loading conditions, giving the model exposure to varied operating scenarios. Figure 10 shows a sample of some of the collected data where subplot (Figure 10a) shows the input current I_{in}, subplot (Figure 10b) shows the diode current I_d, and subplot (Figure 10c) shows the variable of interest; the capacitor current $I_{cap\text{-}rms}$. This data serves as the foundation for the

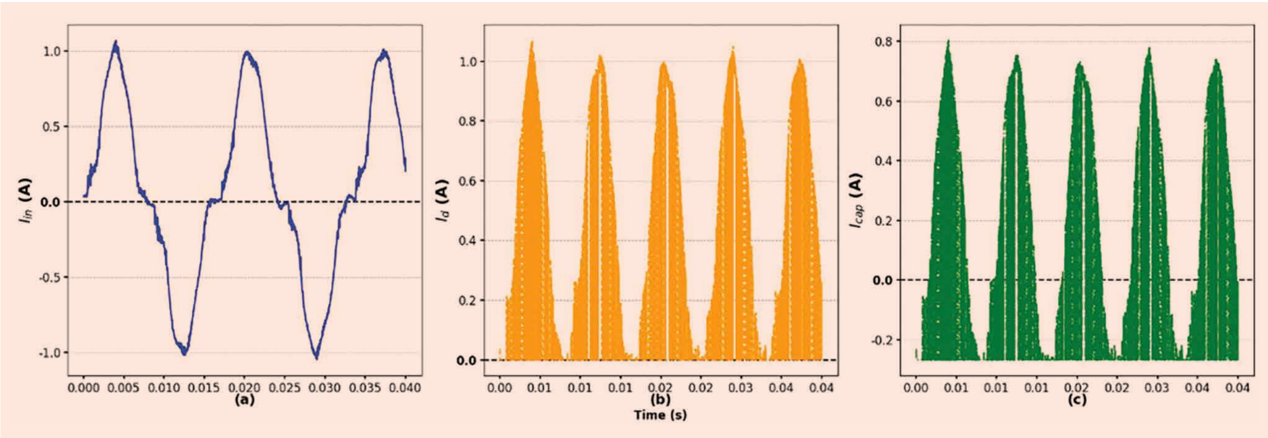

FIG 10 Experimentally measured data from a commercially available 90W PFC stage (see Figure 9). (a) Instantaneous input current (I_{in}) at 90W at 148V. (b) Instantaneous diode current (I_d) computed via MOSFET gate signal on/off. (c) Instantaneous capacitor current (I_{cap}) see (3).

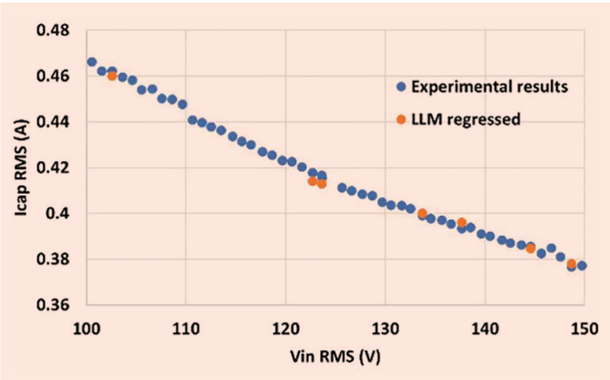

FIG 11 Comparing experimental and predicted values for the experimental FFT fine-tuned predictions for the single-phase boost PFC (Figure 9) capacitor RMS current. Blue dots are captured experimented values while orange dots are predicted using the fine-tuning model.

fine-tuning process, an essential step in enhancing the model's accuracy for predicting ripple currents.

Fine-tuning involves taking a general-purpose Large Language Model (LLM) and adapting it to handle specialized tasks—in this case, predicting $I_{cap\text{-}rms}$ in PFC circuits. The process begins with feeding the model domain-specific data, which it uses to learn the relationships between inputs (like V_{in} and I_{in}) and outputs (like $I_{cap\text{-}rms}$). Through iterative training, the model adjusts its internal parameters to better align its predictions with the task specific data [9], [11].

Fine-tuning not only enhances the model's precision but also allows it to handle complex, nonlinear relationships without additional custom code, making it a highly efficient solution for predictive tasks in power electronics. Figure 11 presents a sample of the LLM's performance, with the predicted capacitor RMS values shown in orange and the experimental values in blue. The fine-tuned LLM model achieves high accuracy, reaching a Mean Absolute Percentage Error of just 0.7% for the capacitor current RMS predictions. A more detailed discussion on this topic is available in [11]

Other Applications for Circuit AI

Circuit AI is equipped with a vast knowledge base derived from multiple rich sources, including academic research and industry standards, ensuring that the AI provides the most accurate and up-to-date information to users. Engineers can rely on Circuit AI to answer conceptual questions about power electronics, such as troubleshooting experiments, understanding and finding equations, and exploring best practices in design (Figure 13). Furthermore, the system can search the internet in real-time, allowing engineers to pull the latest component datasheets, find the most recent research papers, learn about upcoming conferences (Figure 12), and even explore emerging technologies or market trends. This feature empowers users to validate their designs, source alternatives, and gather insights from trusted sources quickly, all through a single interface. By integrating these capabilities, Circuit AI not only streamline design processes but also acts as a comprehensive research assistant, allowing engineers to make well-informed decisions with ease.

With tools like Circuit AI, engineers are empowered to make smarter, quicker decisions, driving innovation and accelerating product development.

Future Works

The future development of Circuit AI will focus on enhancing its integration with industry-standard tools to simplify workflows and improve usability for electronic design engineers. A key priority will be advancing its diagnostic capabilities to enable more accurate fault detection, optimization, and predictive maintenance. Additionally, expanding its knowledge base and introducing more advanced function-calling features will enhance precision, streamline complex tasks, and increase overall productivity. These advancements will empower organizations to achieve greater revenue growth by improving efficiency and optimizing resource utilization.

Circuit AI will allow engineers to dedicate more time to innovative product development rather than

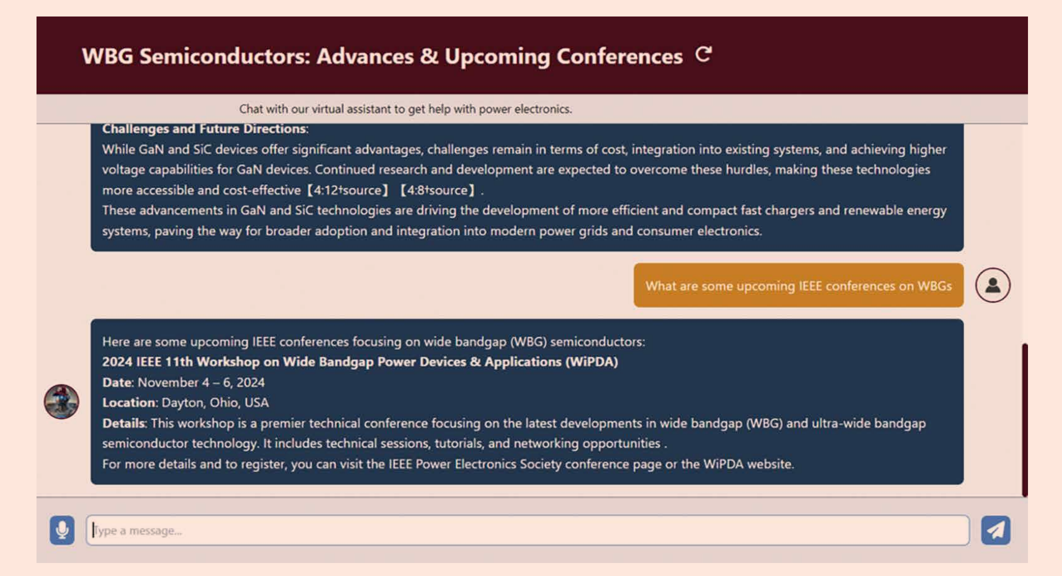

FIG 12 Other applications of Circuit AI: Searching the internet for specific WBG Semiconductor news and latest conferences (results as of 21 September 2024).

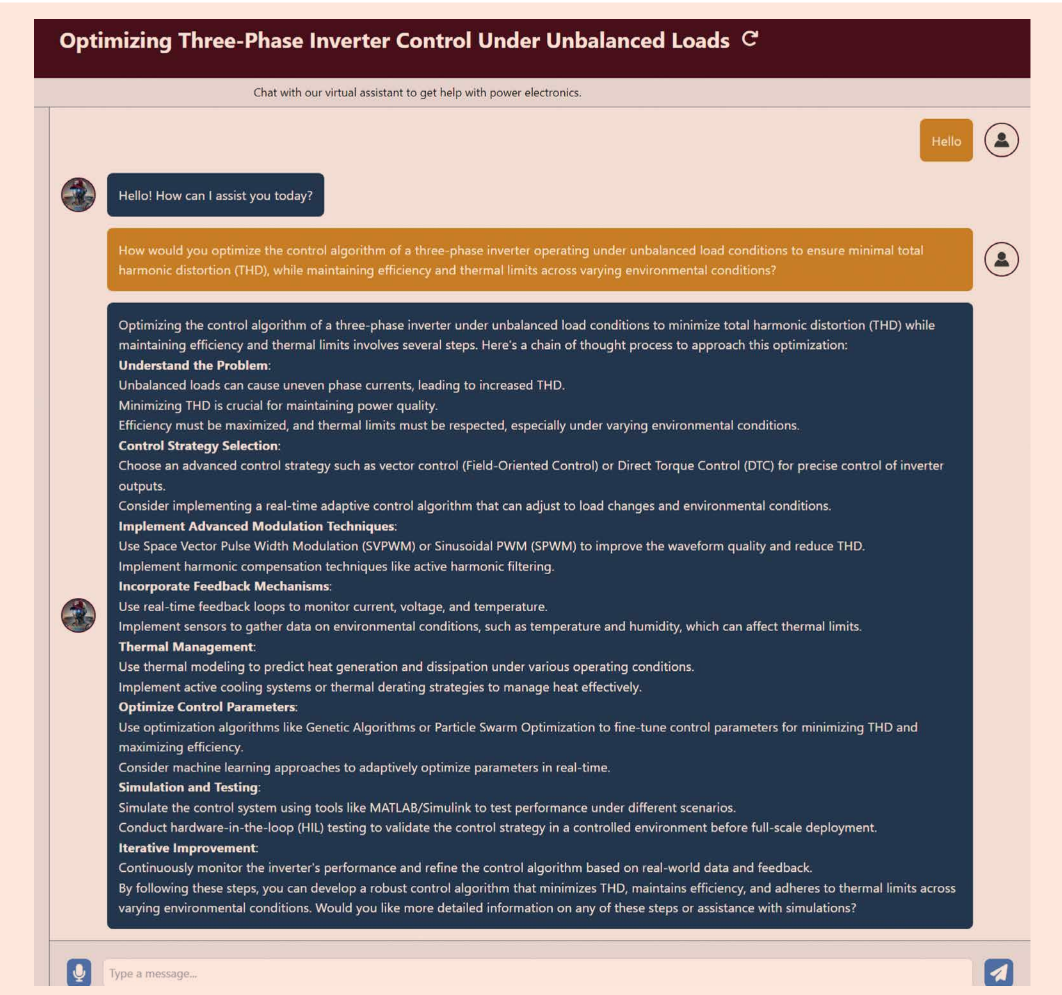

FIG 13 Other applications of Circuit AI: result from the language prompt, "How would you optimize the control algorithm of a three-phase inverter operating under unbalanced load conditions to ensure minimal total harmonic distortion (THD), while maintaining efficiency and thermal limits across varying environmental conditions?"

time-consuming manual processes, fostering greater creativity and progress. Furthermore, these improvements will support in restructuring workflows and aligning organizational processes for maximum productivity. Ultimately, these upgrades aim to establish Circuit AI as a key tool for electronic design automation. By aligning with the innovative methodologies promoted by the PELS community, Circuit AI will contribute to the advancement of power electronics design, driving industry best practices and supporting the evolution of this dynamic field.

Conclusion

The Circuit AI tool has been shown to be a useful tool in the field of power electronics design, streamlining processes that have traditionally been manual and time-consuming. By integrating OpenAI's GPT-4o model with its function-calling, code interpretation, and file search capabilities, Circuit AI has been shown to simplify component selection, optimize BOM costs, and accelerate key calculations like switching and conduction losses. As demonstrated through real-world applications such as the PMP10532 Fly-Buck Power Supply, the tool allows engineers to automate the search for components, can find alternatives, and even compute critical electrical parameters like MOSFET losses. The fine-tuned LLM model has been shown to have high accuracy in predicting the capacitor rms current in PFC circuits.

About the Authors

Vishwam Raval (vishwam@tamu.edu) is currently pursuing the degree in electrical and computer engineering with Texas A&M University, College Station, TX, USA. He is also working on projects that leverage artificial intelligence for various technological applications, including circuit optimization and secure designs. With a strong interest in the intersection of AI and hardware design, he aims to innovate solutions that enhance system efficiency and reliability. His work focuses on integrating advanced methodologies to address contemporary challenges in technology. Driven by a passion for practical research, he is committed to advancing the field of modern technology through innovative approaches and solutions.

Mohamed Zeid (mohamedzeid@tamu.edu) received the bachelor's degree in electrical and computer engineering and the master's degree in computer engineering from Texas A&M University, College Station, TX, USA, where he is currently pursuing the Ph.D. degree in electrical and computer engineering, under the supervision of Prof. Prasad Enjeti. His research interests include power electronics, power quality, control systems, cyber physical systems, and machine learning.

Prasad Enjeti (Fellow, IEEE) (enjeti@tamu.edu) holds the Texas Instruments Jack Kilby Chair Professor and has been at Texas A&M University, College Station, TX, USA, since 1988. An alumnus of Osmania in 1980, IIT Kanpur, and Concordia University, he champions innovative power electronic converter designs and utility interfaces for renewable energy systems (PV/wind/battery) and clean energy systems (fuel cells/supercapacitors/hydrogen), contributing to the field with over 100 journal publications. He has mentored 36 Ph.D. and 53 M.S. graduates, with his doctoral protégés occupying academic and industry leadership roles globally. His research extends to energy conversion systems with wide-bandgap devices, Gen AI applications to power electronics, enhancing cybersecurity, and monitoring in industrial control systems. He is an IEEE Fellow with notable contributions to power electronics.

Grant Pitel (gpitel@magna-power.com) received the B.S. degree in electrical and computer engineering from Cornell University, Ithaca, NY, USA, specializing in digital signal processing, and the M.S. and Ph.D. degrees from the University of Illinois at Urbana-Champaign, Champaign, IL, USA, with a focus on digital control and lithium-ion battery behavior. He is currently the Chief Technology Officer (CTO) with Magna-Power Electronics, Flemington, NJ, USA. As CTO, he oversees all engineering and software activities at Magna-Power, including new product development and internal company technologies. Previously, he served as a Senior Engineer at PC Krause and Associates and interned at Google. He has authored numerous IEEE publications and magazine articles, actively volunteers with IEEE societies IAS and PELS, supports conferences, such as APEC and ECCE, and contributes to the local power electronics chapter in the Philadelphia/Princeton area. Among his accolades are the IEEE IAS Myron Zucker Student Design Award in 2003, the Energy Star Efficiency Challenge Winner in 2004, and the Grainger Outstanding Power Engineer Award in 2005. In 2024, he was inducted into the Ben Franklin Committee on Science and the Arts.

References

[1] *Mouser.* Accessed: Oct. 28, 2024. [Online]. Available: https://www.mouser.com

[2] *Digikey.* Accessed: Oct. 28, 2024. [Online]. Available: https://www.digikey.com

[3] *OpenAI Assistant API Function Calling.* Accessed: Oct. 28, 2024. [Online]. Available: https://platform.openai.com/docs/assistants/tools/function-calling

[4] *Altium Designer.* Accessed: Oct. 28, 2024. [Online]. Available: https://www.altium.com/altium-designer

[5] *Mouser Search API.* Accessed: Oct. 28, 2024. [Online]. Available: https://www.mouser.com/api-search/

[6] *Magna-Power Electronics Inc.* Accessed: Oct. 28, 2024. [Online]. Available: https://magna-power.com/

[7] Tri-Output Fly-Buck Power Supply for Industrial PLC Applications, Texas Instruments. *PMP10532.* PMP10532 Reference Design. Accessed: Sep. 16, 2024. [Online]. Available: http://www.ti.com/tool/PMP10532

[8] N. Mohan, *Power Electronics: Converters, Applications, and Design*, 3rd ed., Wiley, 2003, ch. 2. [Online]. Available: https://www.wiley.com/en-us/Power+Electronics%3A+Converters%2C+Applications%2C+and+Design%2C+3rd+Edition-p-9780471226932

[9] Z. Han et al., "Parameter-efficient fine-tuning for large models: A comprehensive survey," 2024, *arXiv:2403.14608.*

[10] S. J. Castillo, R. S. Balog, and P. Enjeti, "Predicting capacitor reliability in a module-integrated photovoltaic inverter using stress factors from an environmental usage model," in *Proc. North Amer. Power Symp.*, Arlington, TX, USA, Sep. 2010, pp. 1–6, doi: 10.1109/NAPS.2010.5618955.

[11] M. Zeid et al., "Predicting DC-link capacitor current ripple in AC–DC rectifier circuits using fine-tuned large language models," presented at the IECON, Nov. 2024.

PEM